




PAPER

[View Article Online](#)
[View Journal](#) | [View Issue](#)Cite this: *Catal. Sci. Technol.*, 2017, 7, 2838Received 19th April 2017,
Accepted 23rd May 2017

DOI: 10.1039/c7cy00772h

rsc.li/catalysis

Reduction of carbon dioxide and organic carbonyls by hydrosilanes catalysed by the perrhenate anion†

Danny S. Morris,^a Catherine Weetman,^a Julian T. C. Wennmacher,^b Mirza Cokoja,^b Markus Drees,^{} Fritz E. Kühn,^{} and Jason B. Love,^{*}

The simple perrhenate salt $[N(\text{hexyl})_4][\text{ReO}_4]$ acts as a catalyst for the reduction of organic carbonyls and carbon dioxide by primary and secondary hydrosilanes. In the case of CO_2 , this results in the formation of methanol equivalents via silylformate and silylactal intermediates. Furthermore, the addition of alkylamines to the reaction mixture favours catalytic amine *N*-methylation over methanol production under certain conditions. DFT analysis of the mechanism of CO_2 reduction shows that the perrhenate anion activates the silylhydride forming a hypervalent silicate transition state such that the CO_2 can directly cleave a Si–H bond.

Introduction

The hydrosilylation of CO_2 to silylformates and silyl ethers is an attractive route for CO_2 utilisation as, unlike hydrogenation, this reaction is exergonic due to the comparative ease of Si–H bond activation and the strength of the Si–O bond, and the availability of relatively inexpensive and environmentally benign hydrosilanes.^{1–3} A variety of catalysts have been discovered and developed for this reaction, including complexes of Co,⁴ Cu,^{5–8} Ir,^{9–14} Ni,^{15–17} Pd/Pt,¹⁸ Rh,¹⁹ Ru,^{20–25} Sc,²⁶ Zn,^{27–29} and Zr,³⁰ frustrated Lewis pairs,^{31–36} organocatalysts,^{37–42} alkali metal carbonates,⁴³ and even polar solvents such as DMF.³⁸ These reactions result in various reduction products including silyl-formates, -acetals, and -ethers, CO, and methane. This reactivity has been further exploited in a ‘diagonal’ approach to CO_2 reduction/functionalisation, for example in the use of CO_2 as the C1 source for amine *N*-methylation.^{3,37,44–54} High oxidation state transition metal oxo complexes⁵⁵ have been studied in CO_2 reduction chemistry and have been shown to react to form metal carbonates where, in the case of molybdate, the resulting carbonate undergoes hydrosilylation to formate and silylated molybdate, albeit stoichiometrically.^{56–59} Furthermore, rhenium(v) mono and dioxo complexes act as catalysts for the hydrosilylation of organic carbonyls,^{60–65} but this activity is not generally seen for the parent perrhenate, ReO_4^- . Sig-

nificantly, metal oxo complexes have the potential to overcome the oxygen and moisture sensitivity issues from which many current CO_2 hydrosilylation catalysts suffer.

It was shown previously that the pyridinium perrhenate salt $[4,6\text{-Bu}_2\text{C}_5\text{H}_2\text{NH-2-CH}\{(\text{CO})\text{NH}(\text{C}_6\text{H}_{13})\}_2][\text{ReO}_4]$ **1** acts as a catalyst for the epoxidation of alkenes by hydrogen peroxide under biphasic conditions.⁶⁶ Important to this chemistry is the formation of a lipophilic ion pair in which electrostatic and hydrogen-bonding interactions are enhanced in the hydrophobic phase. This catalyst has the advantages of ease of synthesis and manipulation and lack of air-sensitivity, and the recovery of the precious metal is driven by straightforward reverse phase-transfer. Given the efficacy of this new catalyst system and the use of high oxidation state rhenium oxo complexes in reduction catalysis, it is shown here that perrhenate can act as a catalyst for the reduction of carbon dioxide to methanol equivalents by hydrosilanes, that the methylation of alkylamines using CO_2 as the C₁ source occurs under similar catalytic conditions, and that this method can be used to reduce aldehydes and ketones to silyl alcohols.

Results and discussion

Reduction of carbon dioxide

Initially, the reaction between CO_2 (2.5 bar), PhSiH_3 (2.0 mmol), and pyridinium perrhenate **1** (2.0 mol%) at 80 °C in C_6D_6 in a Teflon-tapped NMR tube was monitored by ^1H NMR spectroscopy. However, only 15% consumption of hydrosilane is seen under these conditions after 16 h (Fig. S2 and S3, ESI†). In contrast, when the reaction is carried out using the simple lipophilic quaternary ammonium salt $[N(\text{hexyl})_4][\text{ReO}_4]$ **2** (2.5 mol%) with PhSiH_3 in C_6D_6 at 1 bar of

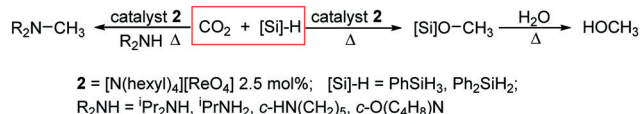
^a EaStCHEM School of Chemistry, University of Edinburgh, David Brewster Road, Edinburgh EH9 3FJ, UK. E-mail: jason.love@ed.ac.uk; Tel: +44 (0)131 650 4762^b Catalysis Research Center, Technische Universität München, Ernst-Otto-Fischer-Straße 1, D-85747 Garching bei München, Germany

† Electronic supplementary information (ESI) available: Full experimental details and spectra. See DOI: 10.1039/c7cy00772h

CO₂ and at 80 °C, complete consumption of the hydrosilane is observed in the ¹H NMR spectrum after 12 h (Fig. S4†) along with the formation of silylformate (3), bis(silyl)acetal (4) and silylated methanol (5) products (Table 1, entry 1 and Scheme 1). Negligible depletion of hydrosilane (<3%) is seen when the reaction is carried out in the absence of CO₂ (under air) for 1 h (Fig. S5 and S6†), confirming that CO₂ is integral to the reaction. This air-stable perrhenate catalyst is also integral as no reaction is seen in the absence of 2 nor in the presence of 5 mol% of N(hexyl)₄Br (Fig. S7†). Increased turnover and selectivity towards methanol equivalents is observed when switching solvents to the more polar CD₃CN (Table 1, entries 3–6). In this case, complete consumption of hydrosilane is observed in 4 h after which the addition of water and heating at 80 °C for a further 2 h results in the formation of methanol, seen as a singlet at 3.28 ppm in the ¹H NMR spectrum (*e.g.* Fig. S9†). Prolonged reaction times to ensure full consumption of all Si–H containing species, *i.e.* no mono/oligomeric siloxyhydride resonances remaining at *ca.* 5.5 ppm, result in an increase in yield of 5. GC-MS analysis of the reduction with Ph₂SiH₂ in CD₃CN prior to quenching indicates the sole presence of Ph₂Si(OMe)₂ confirming that all silylhydrides are consumed in the reaction (Table 1, entry 6, Fig. S60†).

The choice of hydrosilane is important to the reaction as Et₃SiH (Table 1, entry 7) showed no conversion after 24 h at 80 °C, whereas (EtO)₃SiH (Table 1, entry 8) is highly selective towards the formation of silylformate 3, and the use of more sterically demanding Ph₃SiH (Table 1, entry 12) required elevated temperatures. This variation in reactivity is due to a combination of steric inaccessibility of the Si–H bond and the lower Lewis acidity of alkyl silanes.

Further solvent screening found the catalysis to be accelerated in pyridine, with complete hydrosilane consumption observed after 1.5 h (Table 1, entry 9). Using d₇-DMF accelerates the reaction further, with complete hydrosilane depletion after 1 h and an increase in selectivity towards methanol formation compared to the reaction carried out in pyridine (Table 1, entries 10 and 11). Significantly however, reactions in DMF suffer from competitive solvent reduction by hydrosilane to (CD₃)₂NCDH₂, consuming *ca.* 10% of the hydro-



Scheme 1 Reactions of carbon dioxide with hydrosilanes catalysed by the lipophilic perrhenate salt 2.

silane in this process (Fig. S21†). The variation of solvent relates to an increase in turnover frequencies (TOFs), determined from the time taken to consume the hydrosilane at 80 °C, of 3.3 h^{−1} for C₆D₆ to 40 h^{−1} for d₇-DMF. The increase in rate is, in part, due to the increased solubility of CO₂ in the more polar solvent; indeed, a reaction carried out in CD₃CN under 2 bar of CO₂ shows complete hydrosilane depletion within 1.5 h (Fig. S22†).

The longevity of the catalyst system was probed, and at the end of the first catalytic run with Ph₂SiH₂ in d₇-DMF (TOF 40 h^{−1}), the NMR tube was recharged with Ph₂SiH₂ and 1 bar of CO₂ and heated again at 80 °C; this procedure was repeated 3 times. A marginal drop in TOF is observed on the third recharge cycle (36 h^{−1}) after which the reaction was quenched with water and selective formation of methanol is seen (ratio 1:0:99, Fig. S23†). Whilst only a small drop in activity was noted after subsequent recharges, the perrhenate catalyst has significant advantages over current reports due to the ease in which the perrhenate anion can be recovered through simple reverse-phase-transfer techniques.

The faster rate of the reaction in d₇-DMF allowed its monitoring by ¹H and ¹³C NMR spectroscopy at 300 K using ¹³CO₂. On depletion of hydrosilane, broad resonances are seen after 3 h consistent with the formation of silylformate 3 at 8.65 ppm (*d*, *J*_{HC} 219 Hz) and 162.6 ppm (*d*, *J*_{CH} 219 Hz) in the ¹H and ¹³C NMR spectra, respectively (Fig. S24–S29†). After 5 h, quartet resonances at 51.9 ppm (*J*_{CH} 144 Hz) appear in the ¹³C NMR spectrum, consistent with [Si]OCH₃ 5 formation, along with some small triplet resonances at 82.8 ppm (*J*_{CH} 171 Hz) for the bis(silyl)acetal [Si]OCH₂O[Si] 4. In d₇-DMF, the reaction between Ph₂SiH₂ and CO₂ in the *absence* of perrhenate catalyst also leads to silylformate and silylether reduction products in a ratio of 38:62.³⁸ However, this

Table 1 Hydrosilylation of carbon dioxide catalysed by 2.5 mol% [N(hexyl)₄][ReO₄] (2) under 1 bar of CO₂, 0.2 mmol of hydrosilane at 80 °C

	Silane	Time (h)	Solvent	Conversion ^a (%)	Ratio 3:4:5 ^b	TOF ^c (h ^{−1})
1	PhSiH ₃	12	C ₆ D ₆	95	51:18:22	3
2	Ph ₂ SiH ₂	12	C ₆ D ₆	100	73:16:11	3
3	PhSiH ₃	3	CD ₃ CN	96	15:0:85	10
4	Ph ₂ SiH ₂	4	CD ₃ CN	100	16:0:84	13
5	PhSiH ₃ ^d	16	CD ₃ CN	100	2:0:98	3
6	Ph ₂ SiH ₂ ^d	16	CD ₃ CN	100	7:0:93	3
7	Et ₃ SiH	24	CD ₃ CN	0	0	0
8	(EtO) ₃ SiH	24	CD ₃ CN	15	99:0:1	0.3
9	Ph ₂ SiH ₂	1.5	d ₅ -py	100	38:0:62	27
10	PhSiH ₃	1	d ₇ -DMF	100	10:0:90	40
11	Ph ₂ SiH ₂	1	d ₇ -DMF	100	16:0:84	40
12	Ph ₃ SiH ^e	8	d ₇ -DMF	25	21:0:79	1

^a Consumption of hydrosilane. ^b NMR ratio *vs.* Me₃SiPh after water quench. ^c TOF = (conversion/catalyst loading)/time. ^d Prolonged reaction times to consume all Si–H containing species. ^e 150 °C.



background reaction is very slow, taking 144 h to consume the Ph_2SiH_2 at 300 K compared with 10 h when using perrhenate (Fig. S30†).

A series of stoichiometric reactions were undertaken to probe the catalytic mechanism. It was first thought that the mechanism may follow a similar route to the molybdate dianion which reacts initially with CO_2 to form the carbonate complex $\text{Mo}(\text{CO}_3)\text{O}_3^{2-}$; ⁵⁶ however, no reaction of **2** with $^{13}\text{CO}_2$ in the absence of hydrosilane is seen, even after prolonged heating at 80 °C (Fig. S31†), thus ruling out initial carbonate formation in this catalytic cycle. Also, no intermediates are seen in stoichiometric reactions of **2** with varying equivalents of hydrosilane in the absence of CO_2 . It is of note, however, that upon extended heating (>16 h at 80 °C) decomposition of **2** occurs to form trihexylamine, siloxanes and a brown precipitate containing rhenium oxide clusters (Fig. S32–S34†). In light of these experiments, the mechanism of this reaction was evaluated computationally.

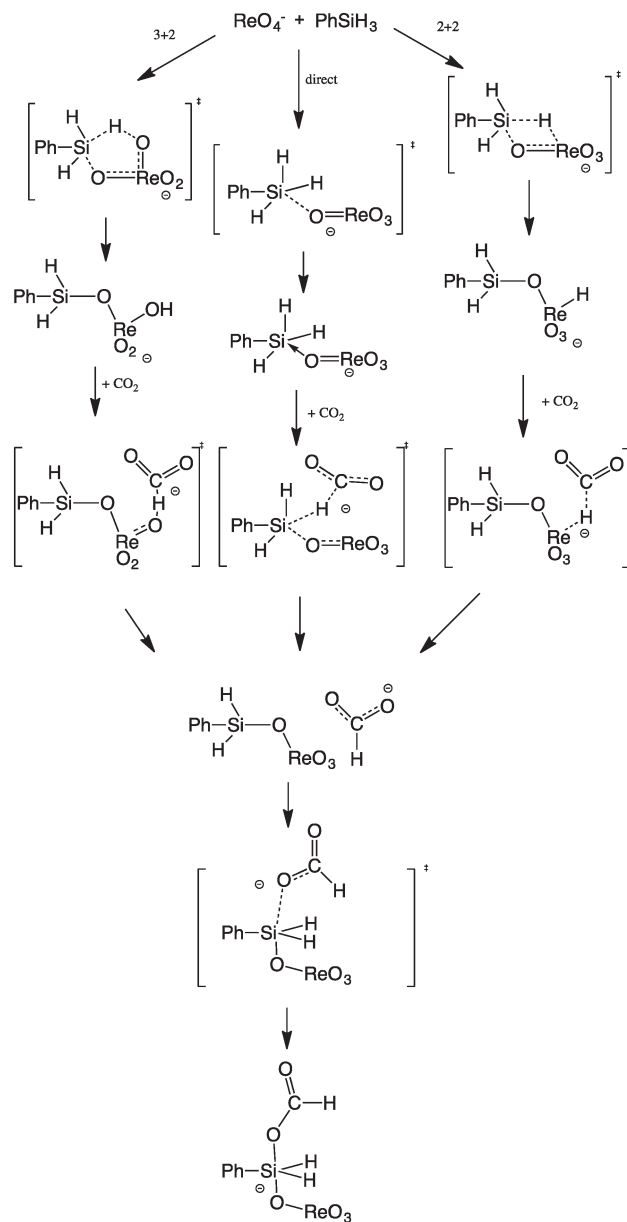
DFT modelling of the catalytic mechanism

To explain how the carbon dioxide reacts with the hydrosilane and the perrhenate catalyst, three different principle pathways have been elucidated (Scheme 2).

Two pathways include activation of the H–Si bond of the relevant hydrosilane by either a [3 + 2] or [2 + 2] cycloaddition to the $\text{Re}=\text{O}$ or $\text{O}=\text{Re}=\text{O}$ fragment of the perrhenate to form a siloxyhydride, with subsequent reaction of this intermediate with CO_2 by hydride migratory insertion. ^{63,65} If Si–H activation would occur to form a hydride, then the most probable mode would be [2 + 2] addition. However, the DFT results favour an alternative ΔG energy profile in the gas phase (Fig. 1) which includes the formation of a simple complex of the hydrosilane with perrhenate without preliminary Si–H activation, forming a five-coordinate hypervalent silicon centre. ^{2,60,67–70} The CO_2 activation occurs then directly at a Si–H bond to form a HCO_2^- species that adds to the silicon to form the observed silylformate (here as adduct of ReO_4^-). This adduct can be seen as a starting point of activating the next Si–H bond by a second CO_2 . In principle, CO_2 can also undergo a cycloaddition to silyl perrhenate intermediates, but the barriers are higher in all pathways. Calculations incorporating a solvent continuum were carried out, with neither benzene nor DMF models significantly altering the preferred mechanism or its energies (see ESI†). Furthermore, alternative mechanisms involving the cycloaddition of CO_2 to a rhenium silicate intermediate were explored, but were found to have higher energy barriers than the route described above (see ESI†).

N-Methylation of amines using carbon dioxide

The observation that silylformates are formed during the catalytic reaction and their implication as intermediates in the N-methylation of amines using CO_2 led us to assess the use of **2** to catalyse this latter reaction. Accordingly, the reaction between CO_2 , HN^iPr_2 , 4 eq. of Ph_2SiH_2 , and 2.5 mol% of **2** at 80 °C in CD_3CN was monitored by ^1H NMR spectroscopy. Af-



Scheme 2 The pathways considered for the DFT investigation of the reduction of CO_2 by hydrosilanes catalysed by the perrhenate salt **2**.

ter 2 h, complete loss of HN^iPr_2 is observed with the concomitant formation of MeN^iPr_2 in quantitative yields (Table 2, entry 1; Fig. S35†). The excess hydrosilane is then consumed in the formation of $[\text{Si}]\text{OCH}_3$ (**5**) as noted by the characteristic resonances in the ^1H NMR spectrum between 3.4–3.6 ppm. The scope of the amine substrate was evaluated, revealing that several aliphatic amines are N-methylated, including isopropylamine (to form $\text{Me}_2\text{N}^i\text{Pr}$), piperidine, pyrrolidine and morpholine (Table 2, entries 2–5). The N-methylation of aromatic primary or secondary amines at this temperature does not occur (Table 2, entries 6 and 7), and instead the hydrosilane is consumed in competitive CO_2 reduction. However, lowering the temperature of reaction negates the further reduction of silylformate by hydrosilane to favour reaction with



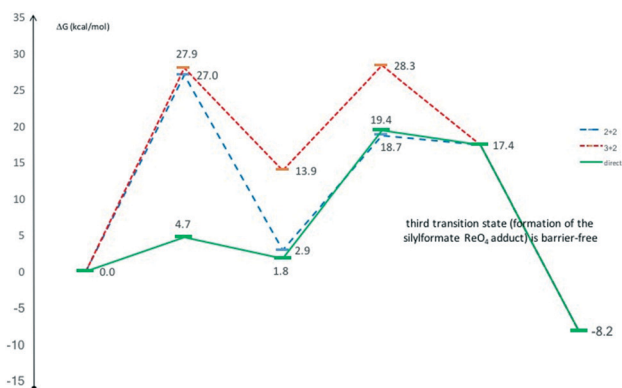


Fig. 1 Calculated Gibbs free-energy profile of the three different pathways.

the poorly nucleophilic *N*-methylaniline and, after 100 h at 20 °C, its conversion to *N,N*-dimethylaniline was seen in 40% yield. Interestingly, the major product of this reaction is the aminal $\text{CH}_2(\text{NMePh})_2$ in 60% yield, seen by its characteristic resonances at 2.86 and 4.78 ppm in the ^1H NMR spectrum (Fig. S41†). Similar aminal formation from CO_2 has been seen previously in organocatalysed or Ru-catalysed reactions.^{47,54} As the aminal can be prepared by the condensation reaction of *N*-methylaniline and formaldehyde, its formation in this catalysed reaction is likely a result of transient formaldehyde production which can arise from the decomposition of $\text{CH}_2(\text{OSiH}_2\text{Ph})_2$.⁷¹

It was reported recently that selective *formylation* of amines is possible using hydrosilanes and CO_2 in polar solvents such as DMF and DMSO.⁷² In contrast, it was found that the simple aliphatic amine HN^iPr_2 underwent *N*-methylation in DMF at room temperature in the absence of 2, and subsequent *in situ* monitoring of this reaction by ^1H NMR spectroscopy found the initial rates essentially identical for the catalysed and uncatalysed reaction (Fig. S40†). Reactions in DMF for the other amine substrates are also selective towards *N*-formylation, which was possible in the absence of 2; however, to achieve *N*-methylation catalyst 2 was required.

Reduction of aldehydes and ketones

Following on from the success of the CO_2 reduction, attention was turned to $\text{C}=\text{O}$ reduction for a variety of carbonyl

containing substrates.^{73–75} An initial trial NMR reaction with benzaldehyde was carried out using the standard reaction conditions of 1.2 eq. of PhSiH_3 , 0.5 mL of CD_3CN and 2.5 mol% of 2 at 80 °C. After 1 h, the ^1H NMR spectrum showed near complete consumption of the aldehyde through loss of the characteristic *CHO* resonance at 10.01 ppm and formation of approximately a 50:50 mixture of $\text{PhSi}(\text{H})(\text{OCH}_2\text{Ph})_2$ and $\text{PhSi}(\text{OCH}_2\text{Ph})_3$; subsequent heating for a further 30 minutes to ensure full consumption of benzaldehyde resulted in no change to the product distribution. Simple hydrolysis through the addition of a small excess of water resulted in full conversion to the benzylalcohol product with concomitant formation of siloxanes (Fig. S42†). Following the same reaction protocol the substrate scope was expanded to other substituted arylaldehydes and alkylaldehydes (Table 3).

The arylaldehyde substrates provided efficient turnover to the corresponding benzylalcohol product upon quenching with water. Aryl substituents containing electron-withdrawing groups (Table 3, entry 2 and 5) proceed with higher TOFs compared to their electron-donating counterparts (Table 3, entry 3 and 4), in line with previous reports of rhenium catalysed hydrosilylation reactions of aldehydes.⁷⁶ In contrast the alkylaldehydes containing more sterically demanding substituents require twice the reaction time in comparison with the linear butyl chain derivatives.

Further extension of this perrhenate hydrosilylation catalysis examined the reduction of ketones (Table 4). Using the same reaction protocol with acetophenone, and monitoring by ^1H NMR spectroscopy, the loss of the singlet resonance for the CH_3 protons at 2.56 ppm is seen after 21 h at 80 °C with three new doublet resonances appearing in the range 1.49–1.37 ppm that correspond to oligomeric $\text{PhCH}_2(\text{O}[\text{Si}])\text{CH}_3$ products; upon quenching with water these resonances resolve into a single species at 1.42 ppm ($J_{\text{HH}} = 6.51$ Hz). The same is also true for the $\text{CH}(\text{O}[\text{Si}])\text{CH}_3$ proton, visible around 5.1 ppm, but due to the oligomeric nature of the silylether products and the overlapping remaining $[\text{Si}]-\text{H}$ resonances this appears as a series of multiplets which resolve into the characteristic quartet at 4.85 ppm ($J_{\text{HH}} = 6.39$ Hz) on quenching. Expanding the scope of this ketone reduction to include substituted acetophenones follows the same trend as observed with the benzaldehyde derivatives. In this case, however, prolonged reaction times are required for the electron-donating substituents, taking 40 h for only 50% consumption

Table 2 *N*-Methylation of amines using 2 bar CO_2 and Ph_2SiH_2 in CD_3CN , heated at 80 °C for 2 h with 2.5 mol% $[\text{N}(\text{hexyl})_4][\text{ReO}_4]$ (2)

	Amine	Hydrosilane (eq.)	NMR yield ^a (%)	TOF (h^{-1})
1	Diisopropylamine	4	99	20
2	Isopropylamine	8	43 ^b	9
3	Piperidine	4	87	17
4	Pyrrolidine	4	82	16
5	Morpholine	4	85	17
6	Aniline	8	0	0
7	<i>N</i> -Methylaniline	4	0	0
8 ^c	<i>N</i> -Methylaniline	4	40	0.4

^a NMR yield vs. Me_3SiPh . ^b $\text{Me}_2\text{N}^i\text{Pr}$. ^c H_3SiPh , 20 °C, 100 h.



Table 3 Hydrosilylation of aldehydes using 1.2 eq. PhSiH₃ in CD₃CN at 80 °C with 2.5 mol% [N(hexyl)₄][ReO₄] (2)

	Aldehyde	Time (h)	NMR yield ^a (%)	TOF ^b (h ⁻¹)
1	Benzaldehyde	1.5	86	23
2	<i>p</i> -Bromobenzaldehyde	1	92	37
3	<i>p</i> -Tolualdehyde	2.5	79	13
4	<i>p</i> -Anisaldehyde	2.5	89	14
5	<i>m</i> -Anisaldehyde	1.5	96	26
6	Trimethylacetaldehyde	4	91	2
7	(1 <i>R</i>)-(-)-Myrtenal	4	47	4
8	Crotonaldehyde	2.5	48	8
9	Butyraldehyde	2	46	9

^a NMR ratio vs. Me₃SiPh after water quench. ^b TOF = (conversion/catalyst loading)/time.

of the starting ketone (Table 4, entries 2 and 4 vs. 3 and 5). Reduction of benzophenone to the corresponding alcohol proceeds efficiently, and again the use of a more sterically demanding alkyl ketone requires prolonged reaction times. Interestingly, a small amount of H/D exchange was seen to take place during extended heating. Hydrogen formation occurs during the initial stages of the reaction where some of the hydrosilane is initially consumed in the reduction of trace water to form H₂ and siloxanes and, in the case of the acetophenone, HD is seen in the ¹H NMR spectrum as a characteristic 1:1:1 triplet at 4.56 ppm (*J*_{HD} = 42.6 Hz) (Fig. S58†). Further H/D exchange was seen at the acetyl position of the acetophenone substrates and is thought to occur through keto–enol tautomerisation in the presence of the [Si]–D which results from the reaction of [Si]–H and D₂O. The use of dry d-solvents negates this HD exchange.

Experimental

Synthesis of [N(hexyl)₄][ReO₄] 2

An aqueous solution of ammonium perrhenate (1.26 g, 4.7 mmol) was added to a chloroform solution of tetrahexylammonium bromide (2.00 g, 4.6 mmol) and stirred together for 6 hours at room temperature after which the two layers were separated and the aqueous layer extracted with chloroform (2 × 10 mL). The combined chloroform extracts were dried over magnesium sulphate and the solvent removed under reduced pressure to provide a colourless solid of tetrahexylammonium perrhenate (2.10 g, 75% yield).

Table 4 Hydrosilylation of ketones using 1.2 eq. PhSiH₃ in CD₃CN at 80 °C with 2.5 mol% [N(hexyl)₄][ReO₄] (2)

	Ketone	Time (h)	NMR yield ^a (%)	TOF ^b (h ⁻¹)
1	Acetophenone	21	72	1
2	<i>p</i> -Bromoacetophenone	40	45	0.5
3	<i>p</i> -Acetyltoylene	21	66	1
4	<i>p</i> -Acetanisole	40	39	0.4
5	<i>m</i> -Acetanisole	20	81	2
6	Benzophenone	21	66	1
7	Pinacolone	37	22	0.2

^a NMR ratio vs. Me₃SiPh after water quench; ^b TOF = (conversion/catalyst loading)/time.

¹H NMR (500 MHz; d₃-MeCN, 300 K): δ_H (ppm) 3.07 (m, 8H, NCH₂), 1.60 (m, 8H, CH₂), 1.33 (m, 24H, CH₂), 0.91 (t, 12H, CH₃).

¹³C{¹H} NMR (500 MHz; d₃-MeCN, 300 K): δ_C (ppm) 59.48 (NCH₂), 31.84 (CH₂), 26.57 (CH₂), 26.57 (CH₂), 23.10 (CH₂), 22.34 (CH₂), 14.21 (CH₃); FTIR (ATR): ν_{max}/cm⁻¹ 902 (Re–O); ESI-MS: M⁺ *m/z* found (calculated): 354.41068 (354.40943 C₂₄H₅₂N₂), 959.77918 (959.75512 (C₂₄H₅₄N)₂ReO₄), 1565.16124 (1565.10132 (C₂₄H₅₄N)₃(ReO₄)₂). M⁻ *m/z* found (calculated): 250.93270 (250.93597 ReO₄), 854.26749 (854.27860 (C₂₄H₅₂N)(ReO₄)₂), 1459.59185 (1459.62427 (C₂₄H₅₂N)₂(ReO₄)₃), 2064.90770 (2064.97026 (C₂₄H₅₂N)₃(ReO₄)₄); analysis: C₂₄H₅₂NO₄Re found (calc.); C: 47.55% (47.65), H: 8.72% (8.67), N: 2.38% (2.32).

General procedure for catalytic reactions of hydrosilanes with CO₂

[N(hexyl)₄][ReO₄] 2 (3 mg, 2.5 mol%) in 0.6 mL d-solvent, hydrosilane (0.2 mmol) and trimethylphenylsilane (2 μL) as an internal standard (unless otherwise stated) were added to a Teflon-tapped NMR tube. The solution was freeze–pump–thaw degassed three times before being refilled with 1 bar of CO₂. The ¹H NMR spectrum was recorded and then the tube was placed in a preheated oil bath (80 °C). The reactions were monitored by ¹H NMR spectroscopy regularly until the hydrosilane was consumed. At this point the reaction was quenched with water (10 μL, 0.56 mmol), heated for 2 h and the ¹H NMR spectrum recorded.

General procedure for catalytic *N*-methylation of amines with CO₂

[N(hexyl)₄][ReO₄] 2 (3 mg, 2.5 mol%) in 0.6 mL d-solvent, amine (0.2 mmol), silane (0.8 mmol) and trimethylphenylsilane (2 μL) as an internal standard (unless otherwise stated) were added to a Teflon-tapped NMR tube. The solution was freeze–pump–thaw degassed three times before being refilled with 2 bar of CO₂. The ¹H NMR spectrum was recorded and then the tube was placed in a preheated oil bath (80 °C) for 2 h, after which the ¹H NMR spectrum was recorded.



General procedure for catalytic hydrosilylation of aldehydes and ketones

[N(hexyl)₄][ReO₄]₂ (3 mg, 2.5 mol%) in 0.5 mL CD₃CN, phenylsilane (0.24 mmol), carbonyl (0.2 mmol) and trimethylphenylsilane (2 µL) as an internal standard were added to a NMR tube. The ¹H NMR spectrum was recorded and then the tube was placed in a preheated oil bath (80 °C). The reactions were monitored by ¹H NMR spectroscopy regularly until the hydrosilane or carbonyl was consumed. At this point the reaction was quenched with water (10 µL, 0.56 mmol), heated for 15 min and the ¹H NMR spectrum recorded.

Computational details

All calculations have been performed with the software Gaussian09.⁷⁷ The hybrid density functional B3LYP^{78–81} has been used together with dispersion correction GD3BJ⁸² and the triple zeta basis set 6-311++G**^{83,84} for all elements except Re. The Re atoms are described with the Stuttgart-Dresden-ECP.⁸⁵ The energies reported are free energies in gas-phase or for the solvents benzene and DMF with SMD solvent calculations at 298.15 K.⁸⁶

Conclusions

We have shown that the simple, lipophilic perrhenate salt [N(hexyl)₄][ReO₄]₂ acts as a catalyst for the reduction of CO₂ by hydrosilanes. This is the first time that perrhenate has acted as a catalyst for CO₂ reduction, and is likely facilitated by dissolution of the lipophilic assembly into a hydrophobic, organic solvent. The calculated mechanism shows that direct attack of CO₂ on a Si–H bond of a perrhenate hypervalent silicate occurs instead of alternative mechanisms through rhenium hydride formation. Furthermore, the observation that *N*-methylation of amines using CO₂ and organic carbonyl reduction can also be undertaken using a perrhenate catalyst expands considerably the scope of this chemistry. The ease of transfer of perrhenate from an organic phase back into an aqueous phase by the addition of base (e.g. NaOH) should lead to straightforward rhenium recycling, an essential step if this precious metal is to be further exploited in catalytic chemistry.

Acknowledgements

We thank the TUM Graduate School, the Johannes Hübner Stiftung (sponsorship of JTCW), the University of Edinburgh and the EPSRC (EP/J018090/1), and the Leibnitz Computing Centre Munich for support.

Notes and references

- 1 F. J. Fernández-Alvarez, A. M. Aitani and L. A. Oro, *Catal. Sci. Technol.*, 2015, 4, 611–624.
- 2 M. Iglesias, F. J. Fernández-Alvarez and L. A. Oro, *ChemCatChem*, 2014, 6, 2486–2489.
- 3 C. Das Neves Gomes, O. Jacquet, C. Villiers, P. Thuéry, M. Ephritikhine and T. Cantat, *Angew. Chem., Int. Ed.*, 2012, 51, 187–190.
- 4 M. L. Scheuermann, S. P. Semproni, I. Pappas and P. J. Chirik, *Inorg. Chem.*, 2014, 53, 9463–9465.
- 5 Y. Tani, K. Kuga, T. Fujihara, J. Terao and Y. Tsuji, *Chem. Commun.*, 2015, 51, 13020–13023.
- 6 K. Motokura, D. Kashiwame, N. Takahashi, A. Miyaji and T. Baba, *Chem. – Eur. J.*, 2013, 19, 10030–10037.
- 7 L. Zhang, J. H. Cheng and Z. M. Hou, *Chem. Commun.*, 2013, 49, 4782–4784.
- 8 K. Motokura, D. Kashiwame, A. Miyaji and T. Baba, *Org. Lett.*, 2012, 14, 2642–2645.
- 9 A. Julian, E. A. Jaseer, K. Garces, F. J. Fernandez-Alvarez, P. Garcia-Orduna, F. J. Lahoz and L. A. Oro, *Catal. Sci. Technol.*, 2016, 6, 4410–4417.
- 10 A. Julian, V. Polo, E. A. Jaseer, F. J. Fernandez-Alvarez and L. A. Oro, *ChemCatChem*, 2015, 7, 3895–3902.
- 11 E. A. Jaseer, M. N. Akhtar, M. Osman, A. Al-Shammari, H. B. Oladipo, K. Garces, F. J. Fernandez-Alvarez, S. Al-Khattaf and L. A. Oro, *Catal. Sci. Technol.*, 2015, 5, 274–279.
- 12 H. B. Oladipo, E. A. Jaseer, A. Julian, F. J. Fernandez-Alvarez, S. Al-Khattaf and L. A. Oro, *J. CO₂ Util.*, 2015, 12, 21–26.
- 13 S. Park, D. Bézier and M. Brookhart, *J. Am. Chem. Soc.*, 2012, 134, 11404–11407.
- 14 T. C. Eisenschmid and R. Eisenberg, *Organometallics*, 1989, 8, 1822–1824.
- 15 P. Rios, N. Curado, J. Lopez-Serrano and A. Rodriguez, *Chem. Commun.*, 2016, 52, 2114–2117.
- 16 L. Gonzalez-Sebastian, M. Flores-Alamo and J. J. Garcia, *Organometallics*, 2013, 32, 7186–7194.
- 17 R. Lalrempuia, M. Iglesias, V. Polo, P. J. S. Miguel, F. J. Fernandez-Alvarez, J. J. Perez-Torrente and L. A. Oro, *Angew. Chem., Int. Ed.*, 2012, 51, 12824–12827.
- 18 S. J. Mitton and L. Turculet, *Chem. – Eur. J.*, 2012, 18, 15258–15262.
- 19 A. J. Huckaba, T. K. Hollis and S. W. Reilly, *Organometallics*, 2013, 32, 6248–6256.
- 20 T. T. Metsänen and M. Oestreich, *Organometallics*, 2015, 34, 543–546.
- 21 P. Deglmann, E. Ember, P. Hofmann, S. Pitter and O. Walter, *Chem. – Eur. J.*, 2007, 13, 2864–2879.
- 22 A. Jansen and S. Pitter, *J. Mol. Catal. A: Chem.*, 2004, 217, 41–45.
- 23 A. Jansen, H. Gorls and S. Pitter, *Organometallics*, 2000, 19, 135–138.
- 24 H. Koinuma, F. Kawakami, H. Kato and H. Hirai, *J. Chem. Soc., Chem. Commun.*, 1981, 213–214.
- 25 G. Süß-Fink and J. Reiner, *J. Organomet. Chem.*, 1981, 221, C36–C38.
- 26 F. A. LeBlanc, W. E. Piers and M. Parvez, *Angew. Chem., Int. Ed.*, 2014, 53, 789–792.
- 27 M. M. Deshmukh and S. Sakaki, *Inorg. Chem.*, 2014, 53, 8485–8493.
- 28 A. Rit, A. Zanardi, T. P. Spaniol, L. Maron and J. Okuda, *Angew. Chem., Int. Ed.*, 2014, 53, 13273–13277.



- 29 W. Sattler and G. Parkin, *J. Am. Chem. Soc.*, 2012, **134**, 17462–17465.
- 30 T. Matsuo and H. Kawaguchi, *J. Am. Chem. Soc.*, 2006, **128**, 12362–12363.
- 31 J. W. Chen, L. Falivene, L. Caporaso, L. Cavallo and E. Y. X. Chen, *J. Am. Chem. Soc.*, 2016, **138**, 5321–5333.
- 32 S. A. Weicker and D. W. Stephan, *Chem. – Eur. J.*, 2015, **21**, 13027–13034.
- 33 R. Dobrovetsky and D. W. Stephan, *Isr. J. Chem.*, 2015, **55**, 206–209.
- 34 Y. Jiang, O. Blacque, T. Fox and H. Berke, *J. Am. Chem. Soc.*, 2013, **135**, 7751–7760.
- 35 M. Khandelwal and R. J. Wehmschulte, *Angew. Chem., Int. Ed.*, 2012, **51**, 7323–7326.
- 36 A. Berkefeld, W. E. Piers and M. Parvez, *J. Am. Chem. Soc.*, 2010, **132**, 10660–10661.
- 37 D. Mukherjee, D. F. Sauer, A. Zanardi and J. Okuda, *Chem. – Eur. J.*, 2016, **22**, 7730–7733.
- 38 M. A. Courtemanche, M. A. Legare, E. Rochette and F. G. Fontaine, *Chem. Commun.*, 2015, **51**, 6858–6861.
- 39 K. Motokura, M. Naito, S. Yamaguchi, A. Miyaji and T. Baba, *Chem. Lett.*, 2015, **44**, 1464–1466.
- 40 C. Lescot, D. U. Nielsen, I. S. Makarov, A. T. Lindhardt, K. Daasbjerg and T. Skrydstrup, *J. Am. Chem. Soc.*, 2014, **136**, 6142–6147.
- 41 S. N. Riduan, J. Y. Ying and Y. G. Zhang, *ChemCatChem*, 2013, **5**, 1490–1496.
- 42 S. N. Riduan, Y. Zhang and J. Y. Ying, *Angew. Chem., Int. Ed.*, 2009, **48**, 3322–3325.
- 43 C. Fang, C. Lu, M. Liu, Y. Zhu, Y. Fu and B.-L. Lin, *ACS Catal.*, 2016, **6**, 7876–7881.
- 44 S. Q. Zhang, Q. Q. Mei, H. Y. Liu, H. Z. Liu, Z. P. Zhang and B. X. Han, *RSC Adv.*, 2016, **6**, 32370–32373.
- 45 T. V. Q. Nguyen, W. J. Yoo and S. Kobayashi, *Adv. Synth. Catal.*, 2016, **358**, 452–458.
- 46 T. V. Q. Nguyen, W. J. Yoo and S. Kobayashi, *Angew. Chem., Int. Ed.*, 2015, **54**, 9209–9212.
- 47 X. Frogneux, E. Blondiaux, P. Thuéry and T. Cantat, *ACS Catal.*, 2015, **5**, 3983–3987.
- 48 L. D. Hao, Y. F. Zhao, B. Yu, Z. Z. Yang, H. Y. Zhang, B. X. Han, X. Gao and Z. M. Liu, *ACS Catal.*, 2015, **5**, 4989–4993.
- 49 Z. Lu, H. Hausmann, S. Becker and H. A. Wegner, *J. Am. Chem. Soc.*, 2015, **137**, 5332–5335.
- 50 O. Santoro, F. Lazreg, Y. Minenkov, L. Cavallo and C. S. J. Cazin, *Dalton Trans.*, 2015, **44**, 18138–18144.
- 51 X. Frogneux, O. Jacquet and T. Cantat, *Catal. Sci. Technol.*, 2014, **4**, 1529–1533.
- 52 O. Jacquet, X. Frogneux, C. Das Neves Gomes and T. Cantat, *Chem. Sci.*, 2013, **4**, 2127–2131.
- 53 O. Jacquet, C. D. Gomes, M. Ephritikhine and T. Cantat, *ChemCatChem*, 2013, **5**, 117–120.
- 54 Y. Li, X. Fang, K. Junge and M. Beller, *Angew. Chem., Int. Ed.*, 2013, **52**, 9568–9571.
- 55 R. G. de Noronha and A. C. Fernandes, *Curr. Org. Chem.*, 2012, **16**, 33–64.
- 56 I. Knopf, T. Ono, M. Temprado, D. Tofan and C. C. Cummins, *Chem. Sci.*, 2014, **5**, 1772–1776.
- 57 J. P. Krogman, M. W. Bezpalko, B. M. Foxman and C. M. Thomas, *Inorg. Chem.*, 2013, **52**, 3022–3031.
- 58 J. S. Silvia and C. C. Cummins, *Chem. Sci.*, 2011, **2**, 1474–1479.
- 59 N. P. Tsvetkov, J. G. Andino, H. Fan, A. Y. Verat and K. G. Caulton, *Dalton Trans.*, 2013, **42**, 6745–6755.
- 60 L. Huang, W. Wang and H. Wei, *J. Mol. Catal. A: Chem.*, 2015, **400**, 31–41.
- 61 P. Gu, W. Wang, Y. Wang and H. Wei, *Organometallics*, 2013, **32**, 47–51.
- 62 S. C. A. Sousa, I. Cabrita and A. C. Fernandes, *Chem. Soc. Rev.*, 2012, **41**, 5641–5653.
- 63 K. A. Nolin, J. R. Krumper, M. D. Pluth, R. G. Bergman and F. D. Toste, *J. Am. Chem. Soc.*, 2007, **129**, 14684–14696.
- 64 G. Du, P. E. Fanwick and M. M. Abu-Omar, *J. Am. Chem. Soc.*, 2007, **129**, 5180–5187.
- 65 E. A. Ison, E. R. Trivedi, R. A. Corbin and M. M. Abu-Omar, *J. Am. Chem. Soc.*, 2005, **127**, 15374–15375.
- 66 M. Cokoja, I. I. E. Markovits, M. H. Anthofer, S. Poplata, A. Pothig, D. S. Morris, P. A. Tasker, W. A. Herrmann, F. E. Kühn and J. B. Love, *Chem. Commun.*, 2015, **51**, 3399–3402; M. D. Zhou, M. Liu, J. Huang, J. Zhang, J. Wang, X. Li, F. E. Kühn and S. L. Zang, *Green Chem.*, 2015, **17**, 1186–1193; I. I. E. Markovits, A. A. Eger, S. Yue, M. Cokoja, C. J. Münchmeyer, B. Zhang, M. D. Zhou, A. Genest, J. Mink, S. L. Zang, N. Rösch and F. E. Kühn, *Chem. Eur. J.*, 2013, **19**, 5972–5979; B. Zhang, S. Li, S. Yue, M. Cokoja, M. D. Zhou, S. L. Zang and F. E. Kühn, *J. Organomet. Chem.*, 2013, **744**, 108–112.
- 67 M. J. Bearpark, G. S. McGrady, P. D. Prince and J. W. Steed, *J. Am. Chem. Soc.*, 2001, **123**, 7736–7737.
- 68 R. Corriu, C. Guérin, B. Henner and Q. Wang, *Inorg. Chim. Acta*, 1992, **198**, 705–713.
- 69 Q. Zhou and Y. Li, *J. Am. Chem. Soc.*, 2015, **137**, 10182–10189.
- 70 M. Oestreich, *Angew. Chem., Int. Ed.*, 2016, **55**, 494–499.
- 71 F. Huang, G. Lu, L. Zhao, H. Li and Z.-X. Wang, *J. Am. Chem. Soc.*, 2010, **132**, 12388–12396.
- 72 H. Lv, Q. Xing, C. Yue, Z. Lei and F. Li, *Chem. Commun.*, 2016, **52**, 6545–6548.
- 73 S. Abbina, S. Bian, C. Oian and G. Du, *ACS Catal.*, 2013, **3**, 678–684.
- 74 T. V. Truong, E. A. Kastl and G. Du, *Tetrahedron Lett.*, 2011, **52**, 1670–1672.
- 75 H. Dong and H. Berke, *Adv. Synth. Catal.*, 2009, **351**, 1783–1788.
- 76 D. E. Perez, J. L. Smeltz, R. D. Sommer, P. D. Boyle and E. A. Ison, *Dalton Trans.*, 2017, **46**, 4609–4616.
- 77 M. J. Frisch, G. W. Trucks, H. B. Schlegel, G. E. Scuseria, M. A. Robb, J. R. Cheeseman, G. Scalmani, V. Barone, B. Mennucci, G. A. Petersson, H. Nakatsuji, M. Caricato, X. Li, H. P. Hratchian, A. F. Izmaylov, J. Bloino, G. Zheng, J. L. Sonnenberg, M. Hada, M. Ehara, K. Toyota, R. Fukuda, J. Hasegawa, M. Ishida, T. Nakajima, Y. Honda, O. Kitao, H. Nakai, T. Vreven, J. A. Montgomery Jr., J. R. Peralta, F.



- Ogliaro, M. Bearpark, J. J. Heyd, E. Brothers, K. N. Kudin, V. N. Staroverov, R. Kobayashi, J. Normand, K. Raghavachari, A. Rendell, J. C. Burant, S. S. Iyengar, J. Tomasi, M. Cossi, N. Rega, J. M. Millam, M. Klene, J. E. Knox, J. B. Cross, V. Bakken, C. Adamo, J. Jaramillo, R. Gomperts, R. E. Stratmann, O. Yazyev, A. J. Austin, R. Cammi, C. Pomelli, J. W. Ochterski, R. L. Martin, K. Morokuma, V. G. Zakrzewski, G. A. Voth, P. Salvador, J. J. Dannenberg, S. Dapprich, A. D. Daniels, O. Farkas, J. B. Foresman, J. V. Ortiz, J. Cioslowski and D. J. Fox, *Gaussian 09*, Gaussian Inc., Wallingford CT, 2009.
- 78 A. D. Becke, *J. Chem. Phys.*, 1993, **98**, 5648–5652.
- 79 C. Lee, W. Yang and R. G. Parr, *Phys. Rev. B*, 1988, **37**, 785–789.
- 80 P. J. Stephens, F. J. Devlin, C. F. Chabalowski and M. J. Frisch, *J. Phys. Chem.*, 1994, **98**, 11623–11627.
- 81 S. H. Vosko, L. Wilk and M. Nusair, *Can. J. Phys.*, 1980, **58**, 1200–1211.
- 82 S. Grimme, S. Ehrlich and L. Goerigk, *J. Comput. Chem.*, 2011, **32**, 1456–1465.
- 83 W. J. Hehre, R. Ditchfield and J. A. Pople, *J. Chem. Phys.*, 1972, **56**, 2257–2261.
- 84 K. Raghavachari, J. S. Binkley, R. Seeger and J. A. Pople, *J. Chem. Phys.*, 1980, **72**, 650–654.
- 85 A. Bergner, M. Dolg, W. Küchle, H. Stoll and H. Preuß, *Mol. Phys.*, 1993, **80**, 1431–1441.
- 86 A. V. Marenich, C. J. Cramer and D. G. Truhlar, *J. Phys. Chem. B*, 2009, **113**, 6378–6396.

